Advances in Nano Research, *Vol. 17, No.1 (2024) 33-49*
https://doi.org/10.12989/anr.2024.17.1.033

Investigation of mechanical surface treatment effect on the properties of titanium thin film

Ehsan Bazzaz*[1], Abolfazl Darvizeh[2a], Majid Alitavoli[2a] and Mehdi Yarmohammad Tooski[3a]

[1]*Department of Mechanical Engineering, Islamic Azad University Central Tehran Branch, Tehran, Iran*
[2]*Department of Mechanical Engineering, University of Guilan, Rasht, Iran*
[3]*Department of Mechanical Engineering, Islamic Azad University South Tehran Branch, Tehran, Iran*

(*Received August 6, 2021, Revised June 21, 2024, Accepted June 27, 2024*)

Abstract. Using the mechanical treatments for mechanical properties improvement was rarely in the development scope before. This research approves through analytical ways that surface impacts can improve the quality of the surface significantly. This fact is approved for deposited titanium on silicone substrate. The new algorithm called minimum resultant error method (MREM) which is a direct combination of nanoindentation, FEM and dimensional analysis through a reverse method is utilized to extract the mechanical characteristics of the coating surface before and after impact. This method is extended to the time dependent behavior of the material to obtain strain rate coefficient. To implement this new approach, a new analysis technic is developed to define the residual stress field caused by surface impact as initial condition for nanoindentation. Analyzing the model in micro and macro scale at the same time was one of the main resolved challenges in this study. The result was obtaining of the constants of Johnson-Cook constitutive equation. Comparing the characteristics of the coating surface before and after impact shows high improvement in yield stress (34%), Elastic modulus (7.75%) and strain hardening coefficient (2.8%). The main achievement is that the strength improvement in titanium thin layer is much higher than bulk titanium. The yield strength shows 41.7% improvement for coated titanium comparing with 24% for bulk material. The rate of enhancement is about 6 times when it comes to the Young's modulus.

Keywords: coating properties; impacted surface; Johnson-cook coefficients; mechanical treatment; micro coatings; minimum resultant error; nanoindentation; surface treatment; titanium coating

1. Introduction

About 40 years ago, when the use of coatings has expanded and become popular, much progress has been made so that the use of a variety of coatings has become inevitable (Herrera *et al*. 2017, dos Santos *et al*. 2007). The range of properties achieved by coatings is very wide, but the main goals of them is to increase the surface hardness and decrease abrasion, along with the improvement of surface lubrication properties (Mamun and Elmustafa 2020). Therefore, this technique is usually used in cutting tools, dental instruments, electronic components, and so on. In the case of cutting tools, the use of Titanium-based coatings increases the life of the tools and helps to reduce the cost of production (Bressan *et al*. 2005, Bulaha and Civcisa 2016).

Improvement of any of above characteristics can lead to a significant achievement in their applications (Altabey 2017). As concluded from comprehensive studies, the subject of the mechanical treatments was rarely investigated by the majority of the researchers. Previous investigations are mostly focused on the effect of the impact (Gauer *et al*. 2017, Ebrahimi and Habibi 2017) and shot peening as the main surface mechanical treatment on the surface properties of pure titanium and its Alloys. Kato *et al*. (1999) proved strengthening of the texture of Ti-6Al-4V and Ludian *et al*. (1999, 2008) showed the effect of both burnishing and shot peening on the quality of Ti-2.5Cu alloy and Titanium Beta C. The same investigation has been repeated by Bae *et al*. (2008) and Maawad *et al*. (2008) for other titanium alloys where they concluded the similar results. The recently finished work of Yang *et al*. (1999) clearly showed the nature of stress and strain distribution under shot peening process. So, there were a few works concerning the pretreatment of the surface of coated materials which is not the matter of our study (Komarov *et al*. 2016, Zhang *et al*. 2016).

It is approved that peening process is generally beneficial for metallic layers intended to fatigue, impact, and wear (Swietlicki *et al*. 2022). This subject is supported by other findings that approve work hardening and residual stress effects on the surface performance after impact (Soyama and Takeo *et al*. 2020). From other viewpoint, some research works were concentrated on the resistance of the coatings against impacts. Qi *et al*. (2022) calculated the resistance of the coated surface under heavy impact. The plastic yielding and plastic strain accumulation during impact process are determined to exhibit the way the heavy impact effect is resisted Qi *et al*. (2023). The effectiveness of the proposed solution method is demonstrated numerically by the finite element method (FEM) and validated by the nano-indentation data. Some others approved that Titanium based coatings such as TiN can

*Corresponding author, Ph.D., Professor,
E-mail: Ehs.Bazaz@iauctb.ac.ir
[a] Ph.D., Professor

ISSN: 2287-237X (Print), 2287-2388 (Online)

effectively improve the protection of the substrate against surface impacts Gsellmann *et al*. (2020). In the most of the previous works, there were very few studies and discussions on the effect of the mechanical treatments on the mechanical properties of the material in coating surfaces. Further investigation should be conducted to clarify the improvement of the mechanical properties of the Titanium coated surface on pure Titanium substrate under surface impact.

The method proposed for the computation of the mechanical properties is developed and applied frequently through a string of research papers by the authors (Bazzaz *et al*. 2019a, b, 2020a). This method is based on a hybrid algorithm that process the output of nanoindentation test to the results of the finite element analysis through a reverse method. The interpretation of the results is done by the MREM algorithm minimizes the errors of the compliance between test and calculation results. Implementation of this complex procedure is applied successfully for obtaining the time dependent properties as well as static properties of pure titanium by Bazzaz *et al*. (2021) In the present paper the similar approach is used for the thin layers on hard substrate in order to calculate the Johnson-Cook coefficients and next to assess the improvement of mechanical characteristics of the coating surface.

Thus, this paper concentrates for the first time on study and investigation of the effect of the mechanical treatments caused by an impact shot on the characteristics of the thin film coatings. For this purpose, a strong computation method has to be proposed to obtain the properties of the coating material before and after the impact. Since the thickness of the PVD coatings is in micro scale and it is too small to be tested by classical most relied test facilities such as Hopkinson bar, a new test method has to be developed for this purpose. The nanoindentation test is utilized in combination with new reverse analysis method as an effective hybrid method to obtain the dependency of the plastic behavior in dynamic-plastic state with the strain rate. A new FEM technic is developed to simulate the whole process including the nanoindentation on row coating surface, plastic impact on coating surface and nano-indentation on impacted coating surface.

2. Finite element model

The Finite Element model has been based on a structure unit that made by means of ABAQUS/Explicit module. The model should be suitable for two stage simulation: impact on the surface and then subsequent nanoindentation test. This can be possible by implementation of step-by-step adjustment in the ABAQUS Code. We will use this novel algorithm for comparison of simulation results with empirical data as main body of a new defined hybrid method. Main part of the model is fabricated from substrate, thin film, the striker and the indenter. Notably, the sample, striker and nano indenter are demonstrated by a cylinder, ball and cone. This ball and cone contribute to simulate the whole model as a cylinder. Since axisymmetric behavior of the substrate is valid, most of researchers (Misra *et al*. 2013, Stauss *et al*. 2003, Karimzadeh *et al*. 2014) considered this assumption in their works, although few researchers employed 3D models in some researches (Dao *et al*. 2001, Antunes *et al*. 2006). So, because of dynamic analysis and existing of huge number of elements and degrees of freedoms, the assumption of 2D model will be too much helpful to decrease the time of each analysis run. As shown by Bazzaz *et al*. (2021) a very slight distinction is detected between both cases by considering after impact residual stress as an adequate measure to compare the results of 2D/3D analysis. The outcomes of 2D mesh solution results are nearer to the preceding solution provided by Yang *et al*. (2018) (Dao *et al*. 2001, Antunes *et al*. 2006), even a negligible difference has been syndicated by the after impact residual stress criterion.

Explicit mode of ABAQUS code should be considered to allow quasi static simulation and dynamic analysis in the same course of calculation run. To obtain the convergence during the solution with high accuracy, it is essential to refine the meshing of the target material. The severe deformation caused by the impact is relatively large respect to the coating film thickness. That is why the refinement of the elements should be reduced gradually from the surface to the far deep elements. So, several researchers considered the total depth of axisymmetric cell as 4 times of the radius of the spherical object (Meguid *et al*. 2002). So, this assumption is examined by the analysis with different impact velocities and it is confirmed that a depth of 2 to 4 times of striker radius is sufficient to reach sufficient accuracy. That is because the stress wave does not have significant effect on the sample for depths more than this depth. According to the fact that a very little thickness is detected in the top thin film compared to whole model depth, some adequate number of elements in the coating layer should be placed so that suitable demonstration of the material behavior is allowed. This is much higher than the number of elements that are necessary for impact analysis (element average size: one tenth to one twentieth of the striker radius) (Sherafatnia *et al*. 2016). In order to model the layer and substrate, a mixture of symmetric triangle/ rectangle elements is put into practice so that the huge size change in the elements is smoothly managed with minimized space. The refinement of the mesh is essential to converge the calculation outcomes and accordingly lessen the analysis calculation errors particularly where the element criterion size is comparable with the indentation depth. It is necessary to refine the surrounding area of the indenter cone tip and zone of the contact with striker to fulfil the requirements of both impact and nanoindentation processes. In this current research, a rectangle basic cell of 5mm×5mm size is sufficient to assure considering all the effects of the dynamic behavior. Mesh size of 1/10 to 1/20 fraction of indentation depth is a good and reliable estimation (Sherafatnia *et al*. 2016). The final meshed model is demonstrated in Fig. 1.

In numerical analysis, the majority of researchers have considered the rigid body assumption for the shot (Meguid *et al*. 2002), although flexible shot was assumed in some of the research works. The reason for that is the assumption of rigid shot can shorten the calculation time with the same accuracy of the results. For Berkovich indenter the model is deliberated as an unadulterated imperfect cone with an

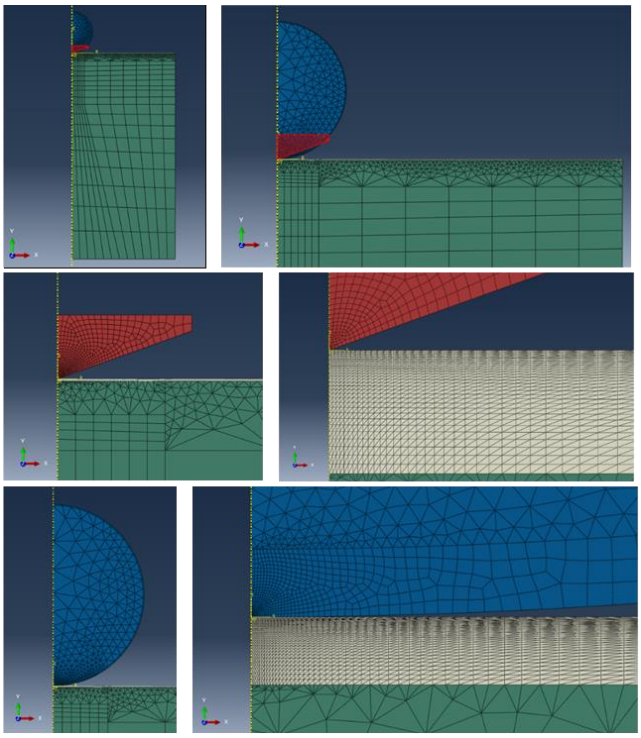

Fig. 1 The meshing including shot, indenter, coating micro layer and base material used for simulation of simultaneous impact and nanoindentation

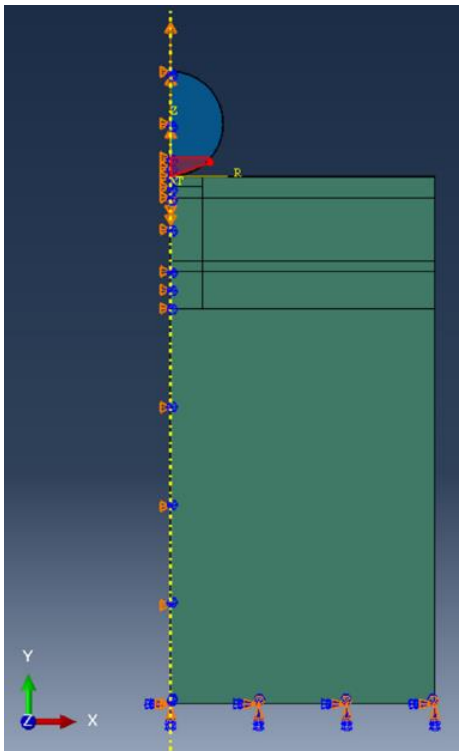

Fig. 2 Symmetric basic cell representation showing all the boundary conditions, initial velocity on the striker and external force applied on the indenter

apical-angle of 170.6 degrees (Lichinchi *et al.* 1998) and zero tip radius in the axisymmetric model. The indenter was typically well-defined as a faultlessly rigid body, it signifies that the distortion in the indenter tip can be abandoned. The output results show no indication of important alteration when it is associated with the Finite Element models with flexible indenters (Sakharova *et al*. 2009) although rigid indenters have been modelled in a lot of researches (Karimzadeh *et al*. 2014). Thus, the indenter is considered as a deformable body to adapt with simultaneous dynamic analysis. With this assumption the real value of Yong modulus can be considered for FEM simulation.

The capability of ABAQUS software allows the contact objects to be defined by sliding surfaces fabricated from contact elements. General contact assumption is considered in some researches to prevent any probable interference with any other parts of the model (Bagherifard *et al*. 2010). This assumption causes more software internal calculations to check any interference between the far away sides of striker and target with contact surfaces. Therefore, only the mating surfaces of the striker and indenter with the target surface are considered. To assure the condition of penetration by indenter and striker, the master face is considered for the mating surfaces of these bodies while the target face is considered as slave. This is the foremost ABAQUS capability that mark a significant advantage than many other Finite Element software (Dassault Systems 2014, Lichinchi *et al*. 1998).

The boundary conditions for the model are well-defined as: all nodes on the substrate base surface are immovable vertical to and parallel with the symmetry axis and all nodes located on symmetry axis are eventually immobile in the vertical angle to the indentation direction. Fig. 2 Displays a general representation of all boundary conditions in the current model cell. In the first stage whereas the simulation is considered as dynamic state the input is defined as the striker velocity. So, regarding the conditions of the loading/unloading procedure during indentation it can be practiced by means of displacement control or load control settings which are permitted through ABAQUS capabilities. Displacement control is more efficient because it provides direct control over the indentation scale (micro- or nano-). Both loadings (dynamic and pseudo static) can be consequently applied by using the capability of ABAQUS to imply different loadings in step-by-step definition in one round of analysis (Dassault Systems 2014).

3. Material behavior and properties

To perform a high-performance coated piece, thin layer coating of titanium is considered on hard substrate of Silicon. When titanium is deposited on Si, the mechanical properties will be changed and even improved, but as a start for the calculations, the properties of bulk titanium will be assumed (Yang and Wang 2018). Since strength of the Silicone substrate is much higher than titanium, the behavior of the Silicone substrate is taken as perfectly plastic material. The commonly used shot peening S230 shot is chosen as striker. As the strength of the shot and substrate are comparable, plastic deformation is expected in both of them. Thus, the behavior of the shot is considered as elastic-perfectly plastic (Yang and Wang 2018). General assumptions of the material characteristics of the substrate,

Table 1 Elastic and plastic material properties of titanium thin layer, Si substrate, shot and diamond indenter

Sample Identification	$E(GPa)$ Young modulus	ν Poisson's ratio	$\sigma_y\ (MPa)$ Yield Stress	$B\ (MPa)$ Strain Hardening Coefficient	n Strain Hardening Exponent
Ti Thin Film	114.8	0.34	304	780.96	0.159
Silicon Substrate	110	0.28	1500	Elastic-Perfectly Plastic	
S230 Shot	200	0.3	1800	Elastic-Perfectly Plastic	
Diamond Indenter	1141	0.07		Full Elastic	

Table 1 Elastic and plastic material properties of titanium thin layer, Si substrate, shot and diamond indenter

α (rad/s)	Mater.	E (GPa)	ρ (kg/m^3)	h (μm)	$\omega_{1,2}$ (rad/s)	α (rad/s)
1404529	Ti	114.8	4500	5	1404529	1404529
31944396	Si	110	2330	5000	31944396	31944396

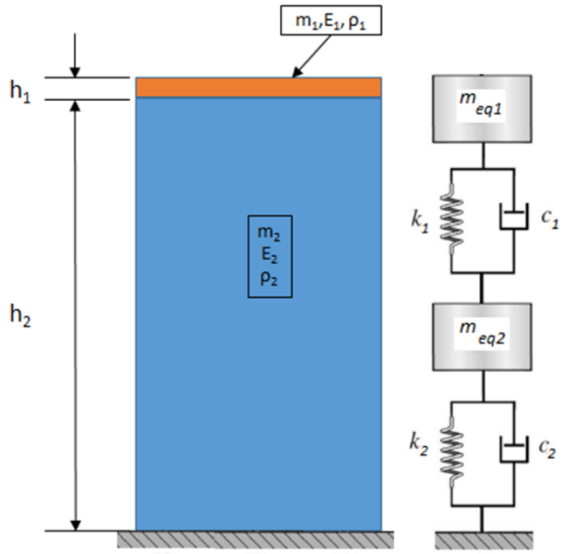

Fig. 3 Simulated two degree of freedom vibration system of the symmetric basic cell of coated material

thin layer, indenter and shot are mentioned according to Table 1.

In order to obtain the material properties of titanium micro layer, nanoindentation test is made on the surface before impact. After finishing of the impact process on the target surface, a residual displacement and consequently stress distribution remains in the sample. Before the residual stress relief, the indenter begins the penetration process on the deformed coating layer to provide a complete nanoindentation data set. Since the simulation is completed in 2 stages: impact and indentation, it is essential to deliberate damping in the dynamic-static model to avert the steady state vibration response which can disturb the precision of the indentation procedure after impact. The ABAQUS recommendation for the coefficient of damping is (Dassault Systems 2014):

$$C = \alpha M + \beta K \tag{1}$$

In which, C, M and K demonstrate the damping matrix, mass matrix and stiffness matrix respectively. So, α and β are mass and stiffness proportional coefficients respectively. The relationship in which the coefficients α and β are related is illustrated by (Ghasemi *et al*. 2016):

$$\zeta_i = \frac{\alpha}{2\omega_i} + \frac{\beta\omega_i}{2} \tag{2}$$

where ζ_i demonstrate the damping ratios relative to the natural frequencies, ω_i. Following relation provides the impact of maximum natural frequency and maximum damping ratio on the time increment in stable state (Dassault Systems 2014):

$$\Delta t \le \frac{2}{\omega_{max}}(\sqrt{1+\zeta_{max}^2} - \zeta_{max}) \tag{3}$$

Obviously, Δt measure is declined by enhancement of ζ_{max} values, hence low analysis time is brought about by selecting the maximum possible damping ratio. As the compound of coating/substrate system can be presumed as a vibrational model of 2 DOF, in which ω_{max} can be obtained as:

$$\zeta_{max} = \frac{\alpha}{2\omega_1} + \frac{\beta\omega_1}{2} \tag{4}$$

Next to some former works (e.g. Meguid *et al*. (2002)), coefficient β can be assumed negligible to decrease total calculation time. Bearing this fact in mind we have:

$$\alpha = 2\omega_1\zeta_{max} \tag{5}$$

In other hand for fast damping and low frequency system (Meguid *et al*. 2002), the maximum damping ratio is designated as 0.5. So, the mass proportional coefficient is obtained: $\alpha = \omega_1$ accordingly. In order to find the first natural frequency, the simulated basic symmetrical cell is simplified as shown in Fig. 3 and then used to obtain the vibration equations and the characteristic equation. Considering a uniform mass and stiffness distribution in all material points, leads to calculation of the equivalent mass and stiffness as follows:

$$\begin{aligned} m_{eq1} &= \frac{1}{3}\rho_1 A h_1, k_1 = E_1 A/h_1 \\ m_{eq2} &= \frac{1}{3}\rho_2 A h_2, k_2 = E_2 A/h_2 \end{aligned} \tag{6}$$

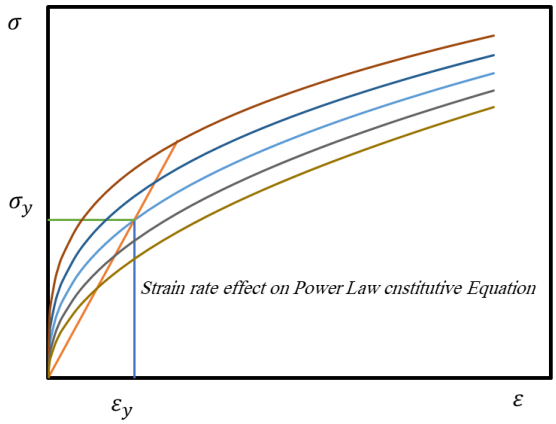

Fig. 4 Representation of Johnson-Cook constitutive equation in the form of power law equation with the dependence to the strain rate

where ρ_i, h_i and E_i are as mentioned in Fig. 3 represent density, height and modulus of elasticity, respectively and *A* represent the area of the basic cell section. By the aid of the characteristic equation, the first and second natural frequencies are calculated as:

$$\omega_{1,2}^2 = \frac{\Omega \pm \sqrt{\Delta}}{2\rho_1\rho_2/3} \tag{7}$$

where the constants are:

$$\Omega = \rho_1\left(\frac{E_1}{h_1 h_2} + \frac{E_2}{h_2^2}\right) + \rho_2\left(\frac{E_1}{h_1^2}\right)$$

$$\Delta = \left[\rho_1\left(\frac{E_1}{h_1 h_2} + \frac{E_2}{h_2^2}\right) + \rho_2\left(\frac{E_1}{h_1^2}\right)\right]^2 - 4\rho_1\rho_2\left(\frac{E_1}{h_1^2}\right)\left(\frac{E_1}{h_1 h_2} + \frac{E_2}{h_2^2}\right) \tag{8}$$

Substituting the physical and mechanical material properties related to the basic cell results in the natural frequencies and mass proportional coefficients as listed in Table 2.

Earlier researches (e.g. Meguid *et al*. 2022) showed that the effect of the friction is negligible on the analysis results. A restraint that prevents the mating surfaces from separation during whole process is developed by the frictionless hypothesis in ABAQUS. Nevertheless, some of the researchers considered a little amount of friction coefficient for steel shots such as 0.1 (Majzoobi *et al*. 2005), 0.2 (Bagherifard *et al*. 2010) and 0.1-0.2 (Frija *et al*. 2006). That is also proved necessary by the analytical results of Sherafatnia *et al*. (2016) to prevent any extra slide over the mating surfaces and for better demonstration of the residual stresses. On the other hand, in nanoindentation procedure, most studies have considered the friction between the indenter outer surface and the substrate (Vaidyanathan *et al*. 2001, Li *et al*. 2013). In some researches, the friction coefficients of 0.1 (Bressan *et al*. 2005) and 0.6 (Karimzadeh *et al*. 2014) are considered for metallic materials. Several researchers have come to this conclusion that the scratch test results can contribute to achieve a relevant estimation for Coulomb friction coefficient (Kot *et al*. 2013). A Hysitron Inc. TriboScope® Nanomechanical test Instrument with 2D transducer, complete software and cube corner diamond indenter was put into practice. The measured lateral force divided by the normal force ratio which has the similar description of friction coefficient can be calculated from the fraction of mean values based on the scratch test output results as 0.413 (Bazzaz *et al*. 2020b). This assessment will be practiced for all cases of FEM analysis in the current research work.

4. Material properties calculation

With the assumption of homogeneous and isotropic behavior, the material properties in the elastic state can be obtained by commonly used method of Oliver and Pharr (1992). As it is well known, the main material properties achieved by using this method are: elastic modulus and the hardness. For this purpose, the parameters of nano-indentation unloading curve slope: $S = dP/dh$ (P is force applied on the indenter and h is penetration depth) and maximum penetration depth h_{max} are all what are required. But when it comes to the obtaining of the plastic properties, there is no straight forward method for computation. Instead, the iteration-based methods utilizing optimization schemes are implemented effectively. To do that, the first step is to consider a behavior pattern or constitutive equation to fit with the material plastic behavior. As one of the most appropriate rules of plastic behavior for majority metallic materials, the power law constitutive equation is commonly used for thin micro film coatings (Wen *et al*. 2017). Fig 4 illustrates the variation of the shape of plastic behavior versus the variation of strain hardening coefficient.

Considering the curves of Fig. 4, the elastoplastic behavior can be tailored with the following form of the power law relation:

$$\sigma = B\varepsilon^n \; for \; \sigma \geq \sigma_y \tag{9}$$

In which σ_y is yield stress whereas *B* and *n* are strain hardening characteristics: coefficient and exponent, respectively. Substituting yield strain from elastic relation and yield stress in the above equation yields the constant B as:

$$\sigma_y = B\left(\frac{\sigma_y}{E}\right)^n$$
$$B = \sigma_y\left(\frac{E}{\sigma_y}\right)^n \tag{10}$$

In the time dependent behavior, the dynamic strain undertakes considerable role in plastic behavior. Fig. 4 shows the effect of the time dependent strain on the material behavior. For such cases, the conventional form of Johnson-Cook constitutive equation: $\sigma = (A + B\varepsilon^n)(1 + Cln\dot{\varepsilon}^*)(1 - T^{*m})$ can be implied. This relation form has been widely used when the metal behavior consists of: strain hardening, time dependent strain and temperature variation effects (Guo and Li 2012). In case the temperature variation can be neglected, the final form of constitutive equation becomes:

$$\sigma = (A + B\varepsilon^n)(1 + C\ ln\frac{\dot{\varepsilon}}{\dot{\varepsilon}_0})\ ,\ T^* = 0 \quad (11)$$

Since A is the yield stress in above equation, therefore it varies in response to the strain rate as follows:

$$\sigma_y = A\left(1 + C\ ln\frac{\dot{\varepsilon}}{\dot{\varepsilon}_0}\right) \quad (12)$$

In which the parameters, $\dot{\varepsilon}$ and $\dot{\varepsilon}_0$ denote the actual and reference (usually 1/s) strain rates, respectively. Combining Eq. (11) and (12) results in the power law form of Johnson-Cook constitutive equations as follows:

$$\sigma = \sigma_y\left[1 + \left(\frac{E}{\sigma_y}\right)^n \varepsilon^n\right]\left(1 + C\ ln\frac{\dot{\varepsilon}}{\dot{\varepsilon}_0}\right) \quad (13)$$

The above equation contains only 3 (σ_y, n, and C) unknown parameters which need to be obtained. The methodology of the combined algorithm is used to obtain the above-mentioned unknown parameters as it is explained in details in Bazzaz *et al*. (2019-2021) previous works. In this methodology, the dimensional analysis is used to provide two dimensionless parameters, ($\frac{K}{E}$, $\frac{W_P}{W_T}$) as demonstrative measures for fitting the FEM analysis to experimental data. As shown in Fig. 5, the parameters K, W_P and W_T are second order coefficient of nanoindentation loading curve, plastic deformation energy and elastic energy, respectively. According to the minimum resultant error algorithm, these parameters are combined to provide a unique criterion to illustrate the difference between analytical and experimental results.

Some of efforts to solve this problem headed to suggest reverse methods and related cooperative algorithms to realize the major necessities of exclusivity during the calculation. Some amendments are applied on the method of dimensional analysis by some researchers (Ma *et al*. 2012a) to adjust it with some consequences found by implement of diverse indenter types. The reverse method planned by Ma *et al*. (2012) was based on Nix-Gao analytical relations between the main parameters: hardness, indentation depth and Young's modulus. Almost all of the reverse methods are using the iteration procedures which lead to the convergence for the majority of metallic materials (Gao *et al*. 2016). When it comes to the comparison between the test data and the calculated data, Noii and Aghayan (2019) have presented a method to optimize and curtail the entire nonconformity. This is done by means of optimization method using point by point deviation between the test data and numerical results.

A specific defined criterion is assumed to combine the errors born by both parameters in order to control the endured problems and assess the errors in more efficient method. Firstly, considering the experimental results as references contributed to express the errors:

$$\mathrm{e(K/E)} = \frac{K^{exp}/\mathrm{E} - K^{num}/\mathrm{E}}{K^{exp}/\mathrm{E}} \quad (14)$$

$$\mathrm{e(W_P/W_T)} = \frac{\mathrm{W_P/W_T|^{exp} - W_P/W_T|^{num}}}{\mathrm{W_P/W_T|^{exp}}} \quad (15)$$

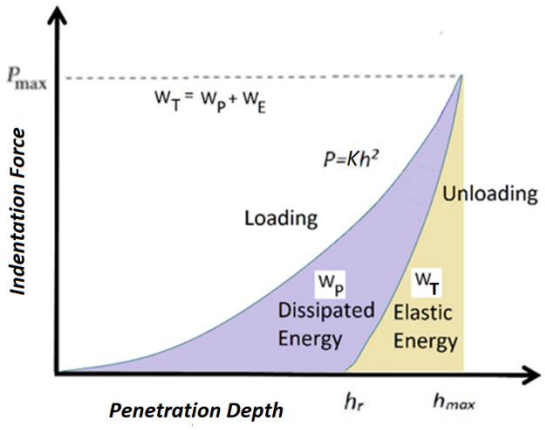

Fig. 5 General indentation force vs penetration depth diagrams drawn by using nanoindentation test data in loading and unloading courses when the creep influence is neglected

where $e(K/E)$ and $e(W_P/W_T)$ are identified as the generated errors of the dimensionless functions. The superscript, num means the data obtained by the numerical analysis whereas exp superscript signifies the experimental data. As a general concept for combining the errors, Wang *et al*. (2010) have proposed to add their absolute values to each other. This supposition appears to be an essential requirement because the magnitudes of the errors have more significant effect than their signs. Additionally, this situation isn't evaluated to provide an adequate measure because both errors are considered with the same order of effect. As such assumption is challenged by the results of many analytical cases, an effective criterion should give a similar signification to both dimensionless parameters. Holistically, a non-metric combination of both errors is planned according to the following relation:

$$\mathrm{e_{rte}} = [Abs[\mathrm{e(K/E)}]^{\mathrm{p}} + Abs[\mathrm{e(W_P/W_T)}]^{\mathrm{p}}]^{1/\mathrm{p}} \quad (16)$$

e_{rte}, is the new introduced total resultant error measure. The appropriate exponent p should be chosen in such a way that the resultant error is minimized. The search for appropriate value of p to achieve this requirement shall be completed case through case. This new defined error criterion is introduced as a single measure to assess the deviation of the experimental data to numerical analysis consequences. The last unique measure is determined as the least value of all resultant total errors of all minima gotten for each set of parameters: B, C and n. According to above definition, this least value is the Infimum of all combined errors which can be conveyed as:

$$\mathrm{(B,C,n)} = \{\mathrm{(B,C,n)}|\mathrm{e_{rte}} = \mathrm{Infimum}(\mathrm{e_{rte}(B,C,n)})\} \quad (17)$$

The method that uses such criterion directly is stated as MREM and applied in this research. Notably, more than one least value may exist over the whole field of all variables which we call them the local minima. Considering the principles based on energy method for determine the yield point, the parameters initiate the first minimum energy level is detected as the set that can start the plastic behavior, henceforth, it will be the required answer. The flow chart

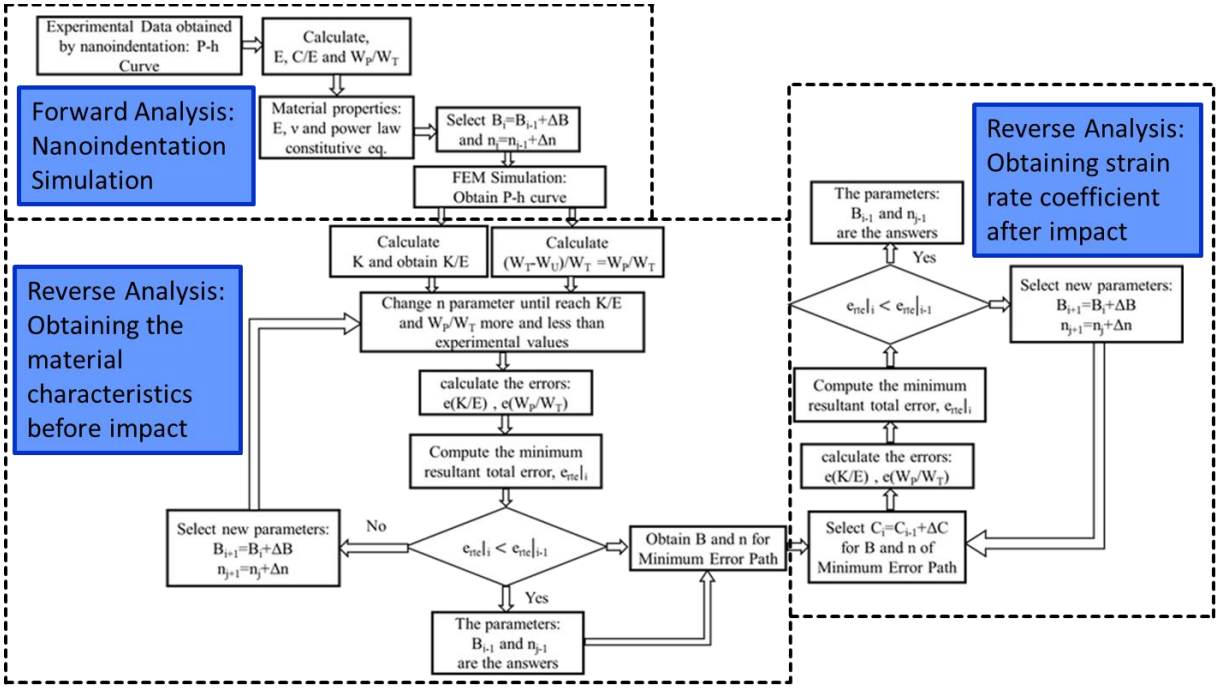

Fig. 6 Flow chart of combined forward and reverse algorithms based on combination of minimum resultant error method and nanoindentation data for obtaining plastic properties in Johnson-Cook equation of coated materials in before and after impact cases

mentioned in Fig. 6 illustrates a process of application of the above-mentioned method (Bazzaz *et al*. 2020b).

The result of implementation the new methodology is obtaining the first four constants of Johnson-Cook constitutive equation for the coating surface after impact. The algorithm is done through a sequence of some following necessary steps:

Step 1. Nanoindentation is applied on the surface of the coating before impact. The elastic properties are obtained by straight forward method and the plastic properties are obtained by reverse analysis.

Step 2. Analysis of the impact and obtaining the plastic effect as a residual stress field.

Step 3. The nanoindentation procedure are done on the deformed and plastically affected coating surface. Nanoindentation curve illustrates the influence of impact on the material mechanical properties.

Step 4. Utilizing the combined algorithm to obtain new mechanical properties after impact.

Step 5. Utilizing the combined algorithm to obtain the coefficient of the strain rate using the same logic of the best fit approach.

5. FEM Simulation

The combined algorithm was verified by the authors utilizing the same data obtained by Yang *et al*. (2018) and Wang *et al*. (2018) for single shot operation. The target was constructed by Pure Titanium with characteristics: 114.8 GPa for elastic modulus and 0.32 for Poisson's ratio. By the same reference when the plastic behavior is considered according to Holloman's constitutive equation the characteristics are 780.95 MPa for strain hardening coefficient and 0.159 for hardening exponent. Utilizing this data, results in the yield stress as 304 MPa. The mechanical properties of the silicone substrate are considered according to Table 1. The striker material is S230 steel ball with 80 m/s velocity and 0.8 mm diameter. The explicit mode of the solver requires non rigid definition for the shot even though the shot was assumed as a rigid body in the main stream of other research works. Therefore, the material of the shot is considered isotropic and linear elastic-plastic. The impact velocity is designated with the purpose of no any damage caused by impact in the substrate. The impact on 3D model generates stress distribution spectrum extended from the surface to the far away depth of the target. As displayed in Fig. 1 it is suggested to use 2D model to diminish the complexity of 3D model. The mesh size is selected to fulfil the requirements of two main categories of the simulation: Nanoindentation as a static behavior and impact as a dynamic behavior. Such consideration is foreseen by investigation of the convergence respect to element size in the former works of the authors and the mesh size is fixed when the results tend to steady value. In the region nearby indenter penetration region where the nanoindentation process is undertaken, the mesh refinement should follow the comments mentioned and verified by the authors.

ABAQUS solver is generally used for simulation of the plastic state behavior (Dassault Systems 2014) in all the stages of the present research. The results of impact implementation on the surface of coating are shown as PEEQ distributions. Fig. 7 shows the situation during the impact of the shot and maximum deformation in the end of impact course. The greatest value of the residual stress distribution is found where the residual deformation is

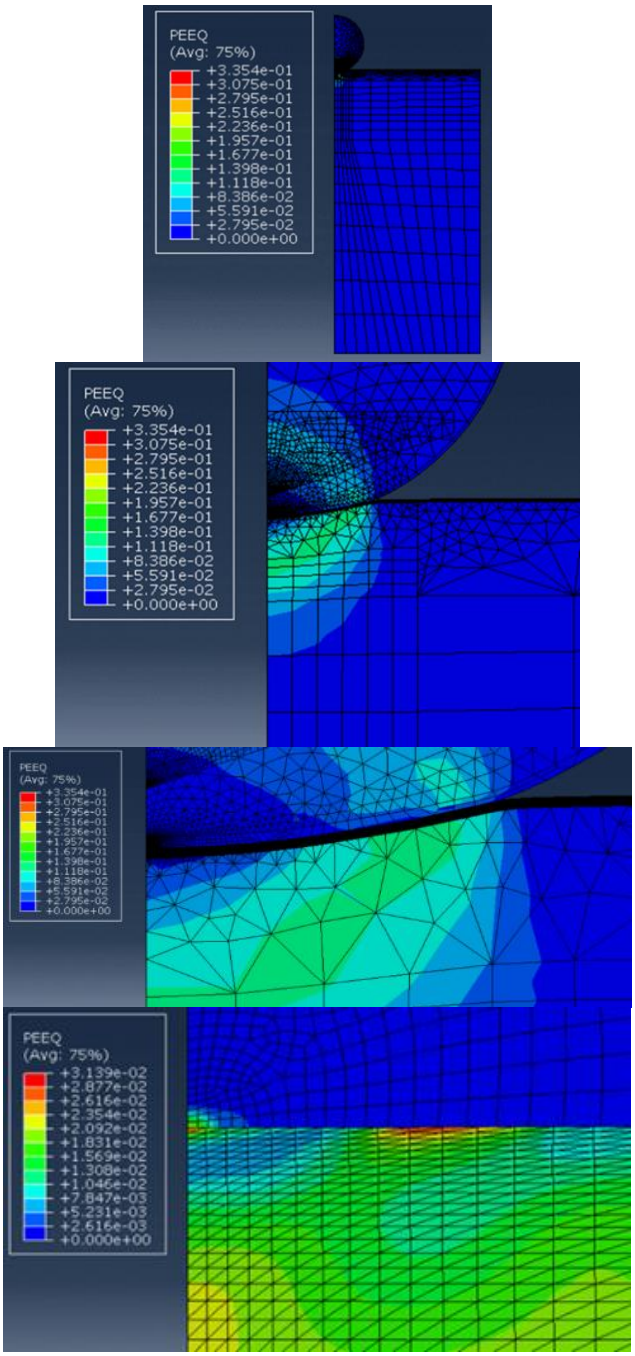

Fig. 7 Equivalent plastic strain distribution caused by shot impact on the silicone target coated by titanium in the maximum deformation situation

thoroughgoing at the impact bump end. When the shot is departed from the target surface during rebound course, it leaves a field of residual stresses and consequent residual plastic deformation nearby collision region as shown in Fig. 8. Study of PEEQ distributions in all cases shows that the plastic deformation is more significant on the target than the shot surface.

The main assumption in the present work is that the imposed impact affects the mechanical properties of the impacted region considerably. To distinguish this effect, the nanoindentation test is considered as an effective means to calculate the final mechanical characteristics coefficients

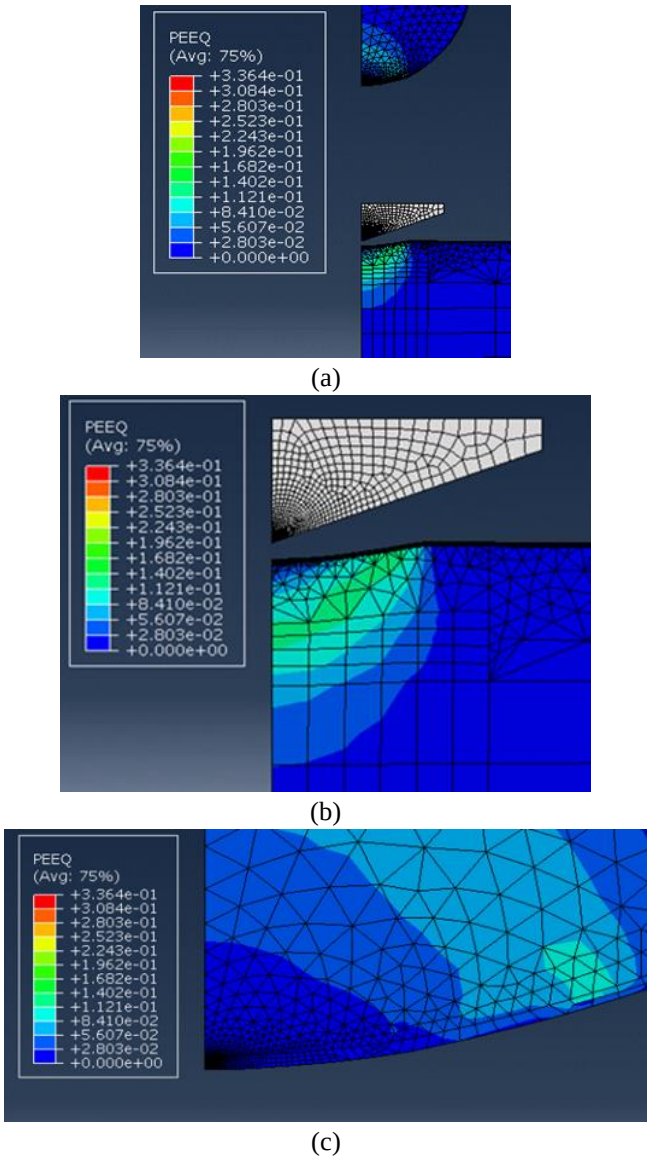

(a)

(b)

(c)

Fig. 8 Equivalent plastic strain distribution in striker and target materials after separation of the shot from target surface. a) The indenter is approaching the target surface after impact to perform nanoindentation measurement. b) The residual stresses are shown more clear after impact. c) Stress distribution in the striker after impact

before and after the impact. Fig. 9 shows the stages of loading, holding, unloading and separation of the indenter on the surface after impact. The penetration of the indenter in the impacted surface, faces more resistance due to the existence of the residual stresses. Knowing the fact that the residual stress distribution in nearby zone of the target upper surface is compressive, explains the increase of the strength in this layer. Comparing the obtained equivalent plastic strain distribution shows this mechanical improvement clearly.

As a result of the nanoindentation process, the P-h curves of nanoindentation before and after impact are shown in Fig. 10. Both curves are the result of the same 400 nm penetration depth to assure that the indentation hole is bigger than the crystal average size significantly (Pelletier

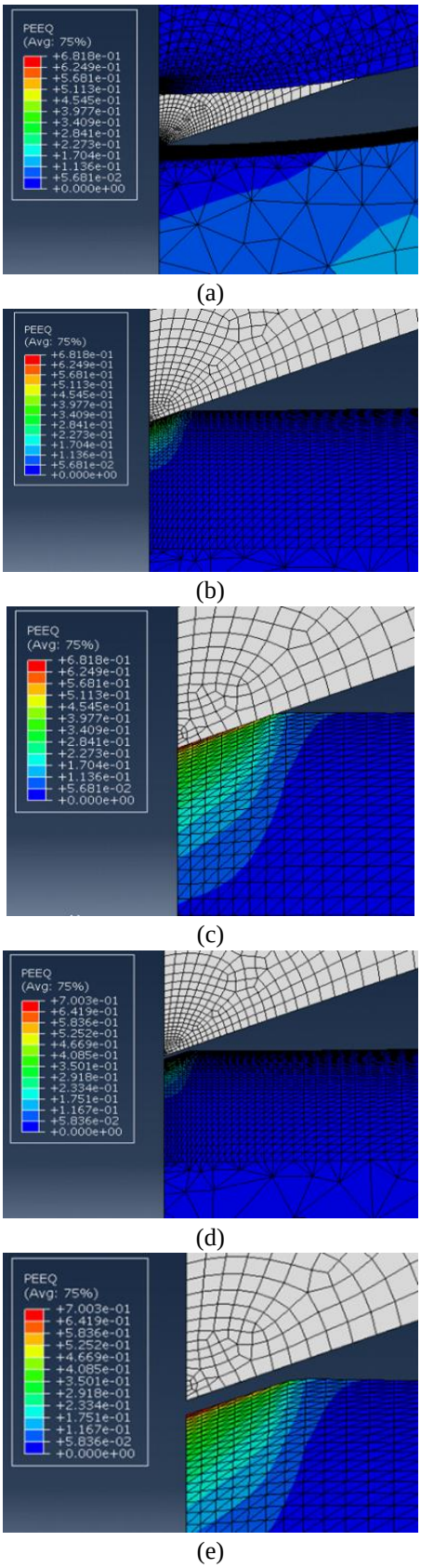

Fig. 9 Nanoindentation stages on the target surface after impact: a) Indenter just contact the target surface, b) The indenter penetration until 400 nm in depth, c) PEEQ distribution caused in maximum deformation, d) Rebound of the indenter e) separation of the indenter from the target surface

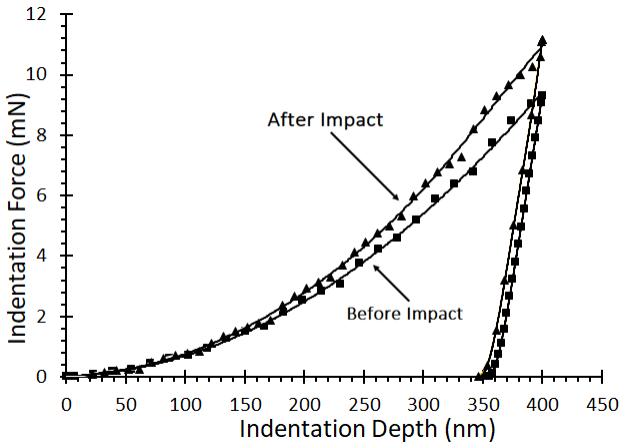

Fig. 10 Force-depth curves born by nanoindentation on the target surface before and after impact

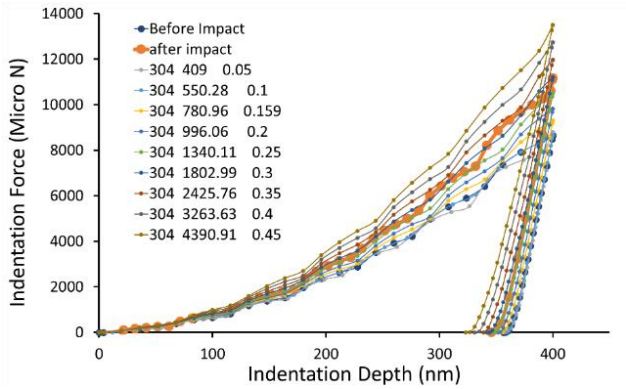

Fig. 11 Indentation force versus penetration depth obtaine by FEM simulation for the data: $\sigma_y = 304$ MPa and n=0 t 0.45 compared with before and after impact curves

et al. 2000, Girleanu *et al*. 2011). Comparing these curves shows a meaningful difference between the situation of before and after impact performance. Young's modulus as the most important material property in the elastic zone is calculated by means of the slope at unloading diagram. Young modulus of the surface before impact coincident with input data but for after impact it shows an increase of 9.3%. The same trend is observed about the parameters K and W_P/W_T as mentioned in Table 3. For simplicity, the ratio of W_P/W_T is substituted by residual indentation depth to maximum indentation depth (h_r/h_{max}) ratio (Dao *et al*. 2001). Difference percentages for the parameters K and h_r/h_{max} are 16% and 12.6%, respectively. This shows significant change relevant to the situation before impact. When it comes to the surface hardening, this change even more and recorded as 22%. Important finding is that improvement of the material properties is also happened because of the substrate effect on the coating thin layer rather than the titanium is used as a bulk material.

6. Plastic material properties

By using the reverse method of Bazzaz *et al*. (2021) known as combined hybrid method, the remained Johnson-

Table 3 Main material and nanoindentation curves characteristics compared for before and after impact cases in titanium thin layer on silicone substrate

Ti Sample case	$E(GPa)$ Coating Modulus of Elasticity	ν Poisson's ratio	H (GPa) Surface Hardness	K Coefficient of Parabolic Curve	h_r/h_{max} Residual depth ratio
Before Impact	113.19	0.34	2.75	59642	0.88355
After Impact	123.7	0.34	3.36	69297	0.99525
Difference Percentage	9.3%	0	22%	16%	12.6%

Table 4 Summary of the calculation of nanoindentation parameters and the parameters required for MREM algorithm (Reference values are taken from after impact curve)

Y	Y/E	n	B	W_P/W_T	K	K/E	W_P/W_T Error	K/E Error	Resultant Error
04	0.0026	0.3	1802.99	0.82176	69998	0.609737	0.013931	0.01010	0.01481
390	0.0034	0.28	1915.80	0.83099	69576	0.606062	0.002856	0.00402	0.00425
400	0.0034	0.14	883.41	0.83284	69471	0.605148	0.000636	0.00250	0.00250
410	0.0035	0.12	806.20	0.83475	69392	0.604459	0.001656	0.00136	0.00182
420	0.0036	0.1	736.07	0.83663	69652	0.606724	0.003912	0.00511	0.00551
430	0.0037	0.08	672.34	0.83855	69753	0.607604	0.006216	0.00657	0.00761
440	0.0038	0.06	614.39	0.84047	69308	0.603728	0.008520	0.00015	0.00852

Cook constitutive equation constants are obtained. These constants are sufficient for demonstration of the plastic behavior of quasi static phenomenon. For this purpose, the main parameters, n and σ_y are variated on the whole domain to allow the minimization of the resultant error. As a primary assumption, the interval 0-0.45 is considered for the exponent of strain hardening and $304\ MPa$ for yield strength. The group set of curves obtained for the variety of the parameters are shown in Fig. 11. As the strain hardening exponent is less than 0.2 in all probable cases, thus the interval of this parameter is limited to this value for upcoming calculations. Yield stress is increased incrementally until all nanoindentation curves become higher than the after-impact curve. For coverage of all the domain of the parameters (n, σ_y), eight group of curves including 72 curves are calculated. Fig. 12 shows all the results of the FEM simulations in separate groups of curves.

The next step in the solution is focused on calculation of K ،W_P and W_T followed by computation of the related dimensionless parameters defined as K/E and W_P/W_T and then the errors of each parameter in comparison to experimental data. A summary of above-mentioned calculations is listed in Table 4. Considering each incremental value of the yield stress, the conditions resulting of the minimum resultant error are obtained. All of these minimum values generate the minimum resultant error path as shown in Fig. 13. Although comparing the individual errors of each dimensionless parameters with each other guides to no specific point for absolutely minimum errors, the variation trend of all resultant error values leads clearly to a unique least point. As seen from Fig. 13, the minimum resultant error of all other minimums is obtained in accordance with $\sigma_y/E = 3.58 \times 10^{-3}$ and related resultant error 0.17%. Other parameters are: yield stress 408 MPa, strain hardening coefficient 802.74 MPa and strain hardening exponent 0.12.

7. Strain rate coefficient

The time dependent Johnson-Cook coefficient, C can be obtained consequently for the coating layer. The method is mainly based on numerical basis regarding MREM method that was successfully used in previous section. The starting point for calculation is the constants of Johnson-Cook equation that obtained for zero strain rate coefficient. Strain rate coefficient is changed incrementally and FEM based calculations are repeated to obtain the relevant P-h nanoindentation curves. The variation domain of C is selected between 0.0 to 0.025 as it is convenient for titanium-based materials. The minimum resultant error and its location is determined of each incremental value of parameter C. This represents an error path that point out the absolutely minimum error value as the final answer.

The methodology is based on important principle that considers the residual stress field after impact as initial condition for nanoindentation. Since this stress field is strongly dependent on plastic and dynamic behavior of given material, the right value of strain rate coefficient undertakes an important task in this procedure. At the commence of solution process, the impact leaves a perpetual distribution of residual stress in the surrounding of the impact implication area. The impact dynamic behavior produces vibration on the whole target including the outer surface of the coating. That is the main reason for the difficulty to allocate the coordinates of the surface before the vibration is completely damped. Although enough damping is considered in the simulation model, but theoretically the vibration is not eliminated completely. Choosing the right calculation frame from ABAQUS results is one of the main challenges to reach more correspondent results. This selection needs some more investigation.

The vibrational response of the model center point as a most displaced point, is divulged in Fig. 14. Reference to

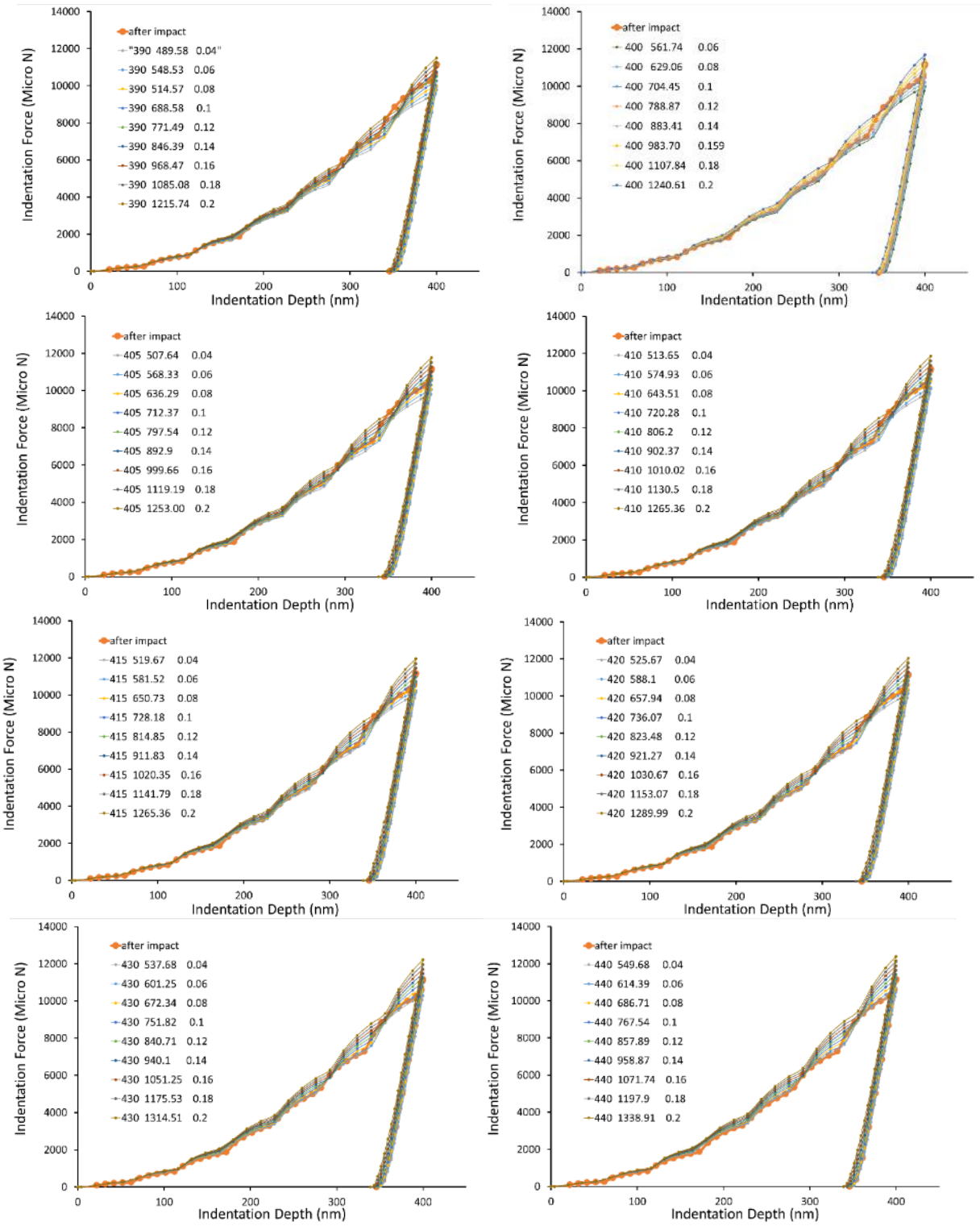

Fig. 12 Indentation force versus penetration depth curves obtained by FEM simulation for incremental variable yield stress and n=0.04 to 0.2 compared with after impact curve

diagram of Fig. 14, the response time is 16μs and the given strain rate is 0.02. To make the vibration amplitude scale visible, it is necessary to draw the diagram for bigger times as the response began from macro displacements and kept on until nano displacements. Graduate magnification of the stated response is displayed in Figs. (14b, c and d). Indeed, by the last diagram Fig. 14d, a maximum variational response almost 1nm is featured for times more than 6μs. Regarding this small response, it is confirmed that any noteworthy outcome on the nanoindentation process is not brought about by the vibration amplitude.

Impact analysis with the conditions of constant speeds and different strain rate coefficients causes different stress conditions for the nanoindentation process which finally

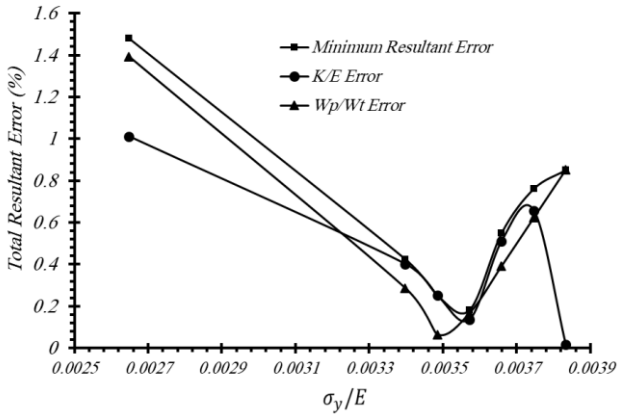

Fig. 13 Variation diagrams of dimensionless parameters *K/E* and W_P/W_T and minimum resultant error versus σ_y/E (for titanium deposited on silicone substrate

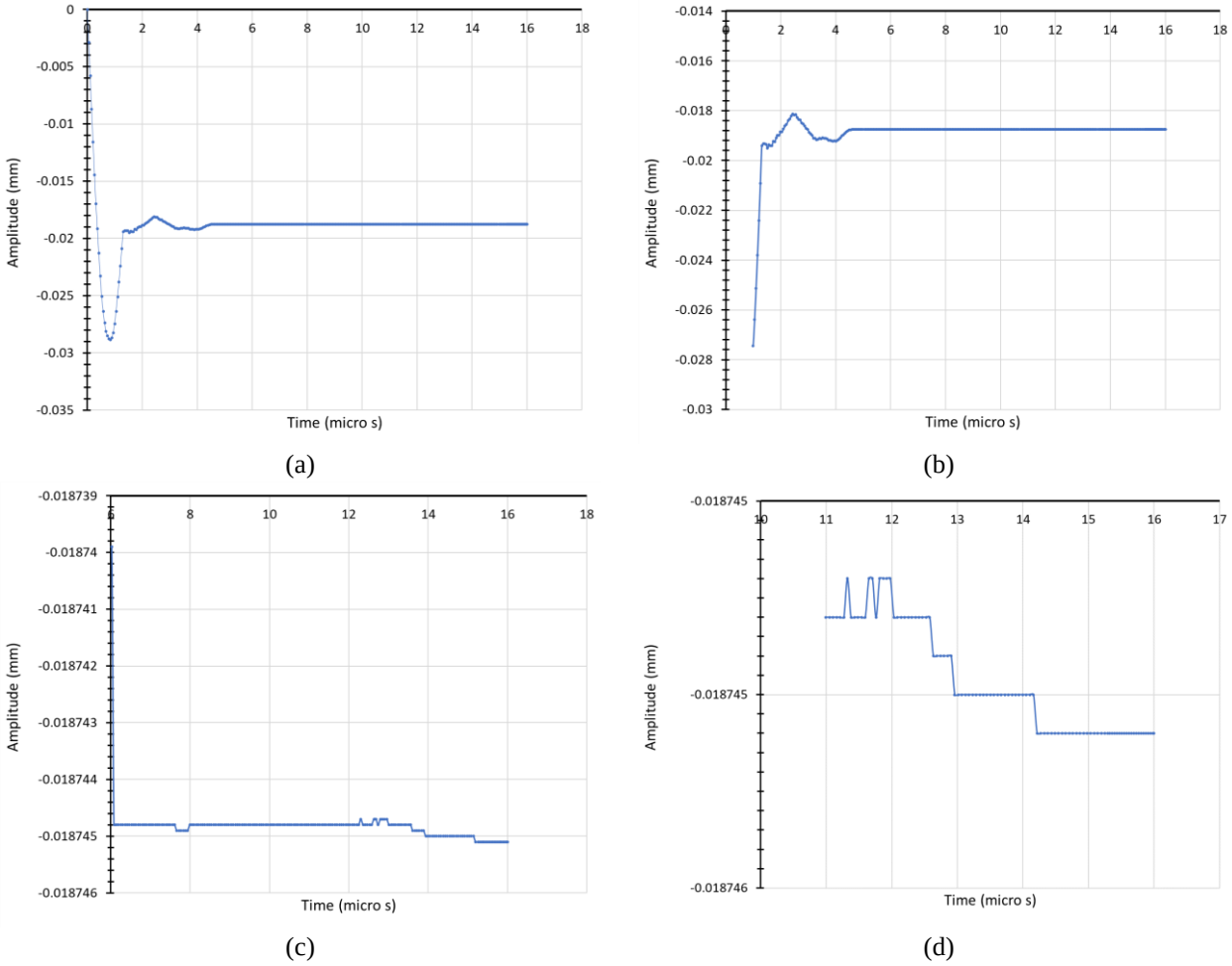

Fig. 14 a) Variation diagram of vibration amplitude versus time under ball striker impact, b) Diagram in the time interval 1-16 µs with maximum magnification, c) Diagram in the time interval 6-16 µs with maximum magnification, d) Diagram in the time interval 11-16 µs with maximum magnification

illustrate meaningful differences in the results. Fig. 15 shows a group of nanoindentation curves with variety of strain rate coefficients in the interval 0.0 to 0.02. Although all curves are very close to each other but their dimension-less parameters *K/E* and W_P/W_T show their difference clearly. According to MREM algorithm, individual errors of each curve are combined to perform the resultant error. Different combination exponent, p values can be selected, but the acceptable one is the one that produce consecutive error less than 1%. Fig. 16 illustrate the trend of consecutive errors versus the combination exponent. To fulfil all above conditions, combination exponent $p=4$ is completely sufficient.

Considering curves of Fig. 15, the minimum resultant

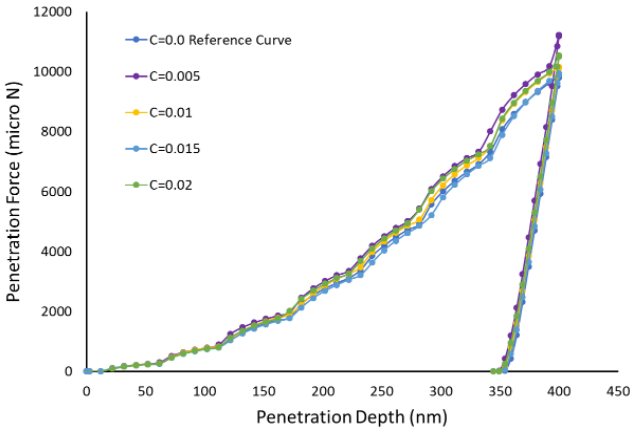

Fig. 15 Nanoindentation curves obtained for the surface after impacts with constant speed and different strain rate coefficients

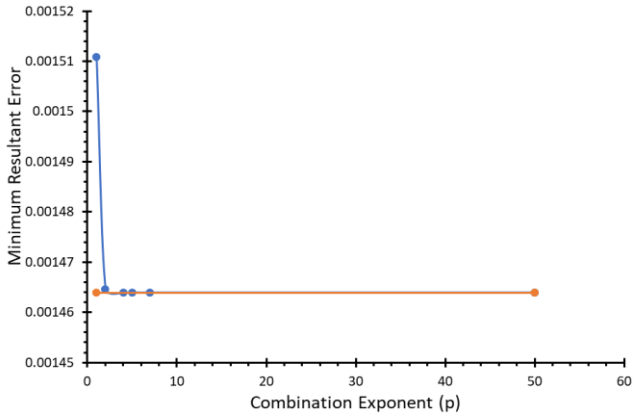

Fig. 16 Variation diagram of the minimum resultant error versus different combination exponent values

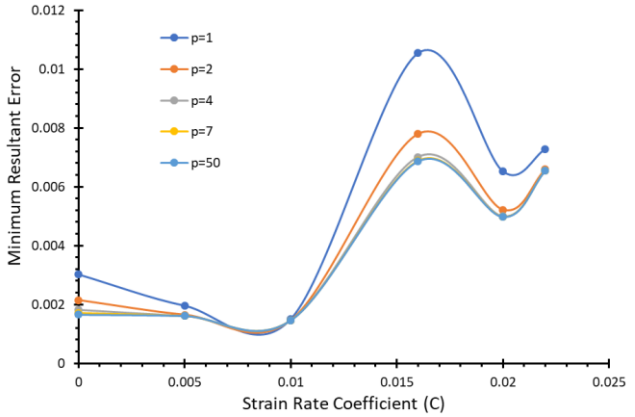

Fig. 17 Minimum resultant error path versus strain rate coefficient for variety of combination exponent. The lowest resultant error value shows the infimum point.

errors for each constant strain rate are calculated and the results are shown for different combination exponents in Fig. 17 diagrams. Study of all diagrams show that all curves tend toward extreme minimum values. The location of this infimum is not dependent to the value of the combination exponents but the value of the resultant error becomes lower when the combination exponent is higher. This infimum point of all resultant errors shown in Fig. 17 is obtained by strain rate 0.009 which is very close to the variety interval of this parameter for pure titanium (Sajadifar and Yapici 2015, Ning *et al.* 2018). On other hand the mechanical properties of pure titanium are available in reference books but for titanium thin layer in micro scale there is no trusted results for comparison.

8. Results and discussion

In purpose of successfully extracting the material plastic properties of bulk materials, the combined MDAM and MREM algorithm have been examined (Bazzaz *et al.* 2019a). Consequently, the influence of the mechanical treatments on the surface characteristics of the bulk titanium is analyzed and evaluated (Bazzaz *et al.* 2019b). To estimate the effect of the same process for coated materials, this algorithm should be extended to conform with the micro and nano scale materials in the same time. The first 3 parameters of Johnson-Cook constitutive equation were calculated for the coating surface before mechanical treatment by using the nanoindentation, whereas the main aim of this research is to achieve the influence of the impact on the above parameters and then to specify the modified coefficient of the strain rate, C. The effect of these parameters has to be determined in the process of the nanoindentation itself because the precision of the indentation data remarkably affect the precision of all modifications made by the new methodology. In order to involve such influences, along with size effects, the penetration depth is predicted in comparison with the crystal structure average size. Thus, taking in account the guidelines born by the research work of Ma *et al.* (2012b), a perfect continuum media behavior can be realized by the consideration of 400 nm penetration depth in the nanoindentation procedure, which is fairly bigger than the typical size of the material structure grains and/or barrels.

Evaluation of the results shows that the mechanical properties before impact can be obtained by static analysis and there is no necessity to consider any strain rate effect. But extracting mechanical properties of the surface after impact requires dynamic solution and consideration of the time dependent parameters. Considering strain rate effect on material behavior is the main assumption that performs the formulation of the new methodology. By using MREM algorithm for both static (Pseudo static) and dynamic cases, it is now possible to extract the material properties of very thin layers without need for very complicated facilities such as Hopkinson bar. With some further efforts and investigations, the new method is capable to be an effective substitution for other conventional methods.

The first achievement of the present work is that the mechanical properties of the soft coating layers on hard substrates can be improved significantly by implementation of the mechanical treatment such as direct impact. Achieved improvement for coating layer is considerably more than what it happened for the bulk materials under the same conditions. This allows us to use the novel materials such as titanium as a coating on cheaper hard materials such as

silicone and achieve more improved characteristics comparing with pure material. The constants of Johnson-Cook constitutive equation as mentioned in Table 5 for cases before and after impact illustrate this fact clearly. The main enhancement can be seen in the yield strength which is the main sign for material strength enhancement. The increase in this parameter is 24% for pure titanium and 34% for titanium coated thin layer on silicone substrate. This means that the enhancement is 41.7% between two previous materials. Thus, using expensive materials such as titanium in the form of thin layer coating results in better characteristics with less cost. At the same time the change in the strain hardening coefficient shows very low rate (2.8%) which reflects the fact that the flexibility of the material remains almost the same. The improvement of the modulus of elasticity is about 6.5% which is almost three times of the pure material.

Studying on preceding research works concentrated on extracting Johnson-Cook constitutive equation constants for pure and titanium-contained materials through experimental measurements indicates that the present data can fully cover their outcome data. About the first 3 parameters of Johnson-Cook constitution equation including Yuong's modulus, Yield strength and strain hardening coefficient, it is obvious that they are common with the time independent behavior parameters (Bazzaz *et al*. 2019a). The results of the former research are used as a start point of the calculations and also as a reference values for comparison of the results as mentioned in the Table 5 (Bazzaz *et al*. 2021). The algorithm of solving the problem was verified for the bulk titanium under impact in former works and can be used safely for the present case.

About the time dependent coefficient, since there is no any trusted data for time dependent plastic properties of titanium thin layer, the other similar cases can be considered. The main issue is the strain rate coefficient which is considered by several researchers in various values for refined grains bulk titanium. By the contribution of the new combined method, some of them are adjacent to the value acquired. The C coefficient has been measured in the range of 0.01 to 0.15 by Ning *et al*. (2018) . In Sajadifar and Yapici (2015) study, strain rate coefficients were found for wide spread temperatures, in which they achieved the values between 0.0055 to 0.02 in the lowermost temperature, 600˚C. As Ti-6Al-4V titanium alloy is the main basis of wide range of Titanium compounds, nearby values 0.0197 (Seo *et al*. 2005) and 0.0198 (Li and He 2006) are dignified. Some others have found most definite values such as 0.014 (Chen *et al*. 2004) and 0.028 (Umbrello 2008). In case of lower weight percent of Titanium compound, e.g. %79.5 wt in Ti6554, *C* coefficient can be higher and were measured as 0.0305 according to Zhan *et al*. (2014)

9. Conclusions

Improving the materials quality of the coating layers is considered as the main purpose of present paper. The material properties improvement by mechanical treatments such as surface impact was not in the aspect of such developments in the past. One of the main achievements of the present research is approving the effectiveness of such treatments to enhance quality of the coating surfaces. Herein, the significance and effects of the surface impact on a titanium thin layer deposited on silicone substrate is studied. Realizing this determination, a methodology is developed through intermingling the outcome results of finite element analysis with an analytical-computational approach. For the first time, a new method is put into practice to implement the nanoindentation on the post impact coating and then analyze the process considering the residual stress distribution as an initial condition. The results were impressive for visualization of the impact effect on the results of the nanoindentation simulation so that the determined deviation could pave the way to estimate the difference of the material properties because of impact implementation.

Previously, the plastic properties of the bulk materials, have been extracted successfully by the joint method of MDAM and MREM algorithms (Bazzaz *et al*. 2019 a, b). The influence of the impact treatment on the surface properties of the bulk titanium is analyzed and evaluated consequently (Bazzaz *et al*. 2020b). To estimate the effect of the same process for coated surfaces, it is necessary to spread expand such algorithm to conform with the micro and nano scale materials in the same time. The most significant purpose of the research is firstly to achieve the influence of any surface impact on three parameters of Johnson-Cook constitutive equation (except temperature) then secondly to calculate the modified strain rate coefficient, C.

Material improvement was perceived under two causes. The first was due to depositing titanium thin layer on a hard substrate and the second was because of the high-rate impact. As the initial sign of such fact, the improvement of the elastic modulus is 1.15% for pure titanium while it is 7.75% for titanium coating. This means that the improvement of the Young's modulus in thin coating layer is more than 5 times regarding to the bulk metal. In order to define the elastic-plastic material behavior to distinguish any probable change in the material physical features, the constitutive equation of Johnson-Cook is designated. The yield stress showed 24.2% improvement for pure titanium while it shows 34% increase for titanium coating. It means more than 41% improvement comparing with pure titanium. When it comes to the strain hardening coefficient, this parameter faces little change about 2.8% for the coated material which shows no big difference in the plastic curve rate. The other main achievement is to practice a novel algorithm by merging the minimum resultant error method with nanoindentation process for pre-impact and post-impact stages. The new method also contributed to obtain the coefficient of strain rate C for the deposited Titanium on hard substrate without need for conventional methods such as Hopkinson bar. Combining the analytical solutions of the nanoindentation process as a static procedure with the impact treatment as a dynamic procedure is another achievement of the present work. A lot of simulation techniques were used to operate such new algorithm.

As the concept that the mechanical treatment has positive surface effect is only believed for the bulk materials and the common belief is that such treatments are not effective for the thin film coatings, we tried to show clearly in the present research that mechanical surface treatment results in considerable enhancement of mechanical behavior and pursuant improvement in the mechanical properties. Consequently, further research should be conducted to show that mechanical surface treatment will not necessarily cause damage on the thin film material structure but make it more dense and tough. Obviously, the next step of the future research will be defining practical ways to imply such treatment on the coated surfaces to finally improve their mechanical properties without increasing the coating film thickness (i.e. using less expensive materials and lower process cost).

Acknowledgement

I would like to thank and appreciate the endeavors of Professor Abolfazl Darvizeh my beloved supervisor which under his acute supervision this research work was carried successfully. But unfortunately, he passed away right after my viva, leaving us in sorrow and deep passion. At any break time, he was surrounded by a large group of students, with whom he was eagerly engaged in serious discussions. He was a devoted supervisor to his research students, many of whom regarded him as their "spiritual mentor". He not only took time to guide them through their research, but also provided them with freedom and opportunity to make their own scientific profile. Peace be upon his sole.

References

Altabey, W. (2017), "An exact solution for mechanical behavior of BFRP nano-thin films embedded in NEMS", *Adv. in Nano Res.*, **5**(4), 337-358. http://doi.org/10.12989/anr.2017.5.4.337.

Antunes, J., Menezes, L. and Fernandes, J. (2006), "Three-dimensional numerical simulation of Vickers indentation tests", *Int. J. Solids Struct.*, **43**(3-4), 784-806. https://doi.org/10.1016/j.ijsolstr.2005.02.048.

ABAQUS 6.14 (2014), *Analysis User's Guide*, Dassault Systems.

Bagherifard, S., Ghelichi, R. and Guagliano, M. (2010), "A numerical model of severe shot peening (SSP) to predict the generation of a nanostructured surface layer of material", *Surf. Coat. Technol.*, **204**(24), 4081-4090. https://doi.org/10.1016/j.surfcoat.2010.05.035.

Bazzaz, E., Darvizeh, A., Alitavoli, M. and Yarmohammad Tooski, M. (2019a), "New hybrid approach in obtaining plastic properties by nanoindentation, finite element method and modified dimensional analysis", *Persian J. Sci. Technol. Compos.*, **6**(3), 451-464. https://doi.org/10.22068/jstc.2019.97778.1497.

Bazzaz, E., Darvizeh, A., Alitavoli, M. and Yarmohammad Tooski, M. (2019b), "Comparing AM200® with titanium-based coatings elastic-plastic properties by nanoindentation, modified dimensional analysis and minimum resultant error method", *Iranian J. Sci. Technol. Transact. Mech. Eng.*, **45**, 197-213. https://doi.org/10.1007/s40997-020-00372-7.

Bazzaz, E., Darvizeh, A., Alitavoli, M. and Yarmohammad Tooski, M. (2020a), "Implementation of the new minimum resultant error approach to extract elastic-plastic properties of titanium nitride thin film by nanoindentation, finite element analysis, and modified dimensional analysis", *Proc IMechE Part C J Mech. Eng. Sci.*, **234**(16), 1-17. https://doi.org/10.1177/0954406220914326.

Bazzaz, E., Darvizeh, A., Alitavoli, M. and Yarmohammad Tooski, M. (2020b), "Investigation of the effect of high rate surface treatment on mechanical properties of titanium base coatings by experimental and numerical analysis", Ph.D. Thesis, University of Guilan, Department of Mechanical Engineering, Rasht, IRAN.

Bazzaz, E., Darvizeh, A., Alitavoli, M. and Yarmohammad Tooski, M. (2021), "A novel method for determination of surface treatment effect on mechanical properties of titanium bulk material", *Proceedings of the Institution of Mechanical Engineers, Part C: Journal of Mechanical Engineering Science*, **236**(1), 382-396. http://doi.org/10.1177/0954406221994881.

Bressan, J., Tramontin, A. and Rosa, C. (2005), "Modelling of nanoindentation of bulk and thin film by finite element method. *Wear*, **258**(1-4), 115-122. http://doi.org/10.1016/j.wear.2004.05.021.

Bulaha, N. and Civcisa, G. (2016), "A comparative study for surface texture evaluation of TiAlN coatings", *Mater. Today Proceedings*, **3**, 2766-2771. https://doi.org/10.1016/j.matpr.2016.06.025.

Chen, L., El-Wardany, T. and Harris, W. (2004), "Modelling the effects of flank wear land and chip formation on residual stresses", *CIRP Annals Manuf. Technol.*, **53**(1), 95-98. https://doi.org/10.1016/S0007-8506(07)60653-2.

Dao, M., Chollacoop, N.V., Van Vliet, K.J., Venkatesh, T.A. and Suresh, S.J.A.M. (2001), "Computational modeling of the forward and reverse problems in instrumented sharp indentation", *Acta Mater.*, **49**(19), 3899-3918. http://doi.org/10.1016/S1359-6454(01)00295-6.

Dos Santos, J.A.B.O., Sales, W.F., Santos, S.C., Machado, A.R., da Silva, M.B., Bonney, J. and Ezugwu, E.O. (2007), "Tribological evaluation of TiN and TiAlN coated PM-HSS gear cutter when machining 19MnCr5 steel", *Int. J. Adv. Manuf. Technol.*, **31**, 629-637. https://doi.org/10.1007/s00170-005-0242-3.

Ebrahimi, F. and Habibi, S. (2017), "Low-velocity impact response of laminated FG-CNT reinforced composite plates in thermal environment", *Adv. Nano Res.*, **5**(2), 69-97. http://doi.org/10.12989/anr.2017.5.2.069.

Frija, M., Hassine, T., Fathallah, R., Bouraoui, C., Dogui, A. and de Génie Mécanique, L. (2006), "Finite element modelling of shot peening process: prediction of the compressive residual stresses, the plastic deformations and the surface integrity", *Mater. Sci. Eng. A*, **426**(1-2), 173-180. https://doi.org/10.1016/j.msea.2006.03.097.

Gao, X., Ma, Z., Jiang, W., Zhang, P., Wang, Y., Pan, Y. and Lu, C. (2016), "Stress strain relationships of LixSn alloys for Lithium ion batteries", *J. Power Sourc.*, **311**, 21-28. http://doi.org/10.1016/j.jpowsour.2016.02.024.

Gauer, K., Dwivedi, M. and Bhatnagar, N. (2017), "Design and analysis of low velocity impact on thermoplastic hat section with curvilinear profile", *Adv. Mater. Res.*, **6**(1), 65-78. https://doi.org/10.12989/amr.2017.6.1.065 65.

Ghasemi, A., Hassani-Gangaraj, S.M., Mahmoudi, A.H., Farrahi, G.H. and Guagliano, M. (2016), "Shot peening coverage effect on residual stress profile by FE random impact analysis", *Surface Eng.*, **32**(11), 861-870. http://doi.org/10.1080/02670844.2016.1192336.

Girleanu, M., Pac, M.J., Louis, P., Ersen, O., Werckmann, J., Rousselot, C. and Tuilier, M.H. (2011), "Characterisation of nano-structured titanium and aluminium nitride coatings by indentation, transmission electron microscopy and electron energy loss spectroscopy", *Thin Solid Films*, **519**(18), 6190-

6195. http://doi.org/10.1016/j.tsf.2011.04.113.
Gsellmann, M., Klünsner, T., Mitterer, C., Marsoner, S., Skordaris, G., Bouzakis, K., Leitner, H. and Ressel, G. (2020), "Near-interface cracking in a TiN coated high speed steel due to combined shear and compression under cyclic impact loading", *Surface Coat. Technol.*, **394**(25), 125854. http://doi.org/10.1016/j.surfcoat.2020.125854
Guo, Y. and Li, Y. (2012), "A novel approach to testing the dynamic shear response of Ti-6Al-4V", *Acta Mechanica Solida Sinica*, **25**(3), 299-311. http://doi.org/10.1016/S0894-9166(12)60027-5.
Herrera, R., Kryshtab, T., Adame, J. and Kryvko, A. (2017), "ZnO thin films with Cu, Ga and Ag dopants prepared by ZnS oxidation in different ambient", *Adv. Nano Res.*, **5**(3), 193-201. http://doi.org/10.12989/anr.2017.5.3.193.
Johnson, K.L. (2012), *Contact Mechanics*. Cambridge University Press. https://doi.org/10.1017/CBO9781139171731
Karimzadeh, A., Ayatollahi, M. and Alizadeh, M. (2014), "Finite element simulation of nano-indentation experiment on aluminum 1100", *Comput. Mater. Sci.*, **81**, 595-600. https://doi.org/10.1016/j.commatsci.2013.09.019.
Kato, Y., Takafuji, S. and Hasegawa, N. (1999), "Effect of small artificial defects and shot peening on fatigue strength of Ti-6Al-4V alloys at elevated temperatures", *Proceedings of the International Conference on Shot Peening*, Tokyo, Japan.
Komarov, F.F., Konstantinov, V.M., Kovalchuk, A.V., Konstantinov, S.V. and Tkachenko, H.A. (2016), "The effect of steel substrate pre-hardening on structural, mechanical, and tribological properties of magnetron sputtered TiN and TiAlN coatings", *Wear*, **92-101**, 352-353. https://doi.org/10.1016/j.wear.2016.02.007.
Kot, M., Rakowski, W., Lackner, J. and Major, L. (2013), "Analysis of spherical indentations of coating-substrate systems: Experiments and finite element modeling", *Mater. Des.*, **43**, 99-111. https://doi.org/10.1016/j.matdes.2012.06.040.
Lichinchi, M., Lenardi, C., Haupt, J. and Vitali, R. (1998), "Simulation of Berkovich nanoindentation experiment on thin films using the finite element method", *Thin Solid Films*, **312**, 240-248. https://doi.org/10.1016/S0040-6090(97)00739-6.
Li, L. and He, N. (2006), "A FEA study on mechanisms of saw-tooth chip deformation in high speed cutting of Ti-6-Al-4V alloy", *Proceedings of the Fifth International Conference on High Speed Machining (HSM)*, Metz, France, 759-767.
Li, W., Huang, C., Yu, M. and Liao, H. (2013), "Investigation on mechanical property of annealed copper particles and cold sprayed copper coating by a micro-indentation testing", *Mater. Des.*, **46**, 219-226. https://doi.org/10.1016/j.matdes.2012.10.029.
Ludian, T., Atoura, J. and Wagner, L. (2008), "Influence of shot peening and burnishing on smooth and notched fatigue strengths of titanium alloys", *Proceedings of the International Conference of Shot Peening 10*, Tokyo, Japan.
Maawad, E., Brokmeier, H.G. and Wagner, L. (2008), "Residual stress-induced subsurface fatigue crack nucleation in shot peening titanium alloys", *Proceedings of the International Conferrence of Shot Peening-10*, Tokyo, Japan.
Majzoobi, G., Azizi, R. and Alavi Nia, A. (2005), "A three-dimensional simulation of shot peening process using multiple shot impacts", *J. Mater. Process. Technol.*, **164-165**, 1226-1234. https://doi.org/10.1016/j.jmatprotec.2005.02.139.
Mamun, M. and Elmustafa, A. (2020), "Fracture toughness of amorphus SiC thin films using nanoindentation and simulation", *Adv. Mater. Res.*, **9**(1), 49-62. http://dx.doi.org/10.12989/amr.2020.9.1.049.
Ma, Z., Zhou, Y., Long, S. and Lu, C. (2012a), "An inverse approach for extracting elastic plastic properties of thin films from small scale sharp indentation", *J. Mater. Sci. Technol.*, **28**(7), 626-635. https://doi.org/10.1016/S1005-0302(12)60108-X.
Ma, Z., Zhou, Y., Long, S. and Luc, C. (2012b), "On the intrinsic hardness of a metallic film/substrate system: indentation size and substrate effects", *Int. J. Plastic.*, **34**,1-11. https://doi.org/1-11.10.1016/j.ijplas.2012.01.001.
Ma, Z.S., Zhou, Y.C., Long, S.G., Zhong, X.L. and Lu, C. (2012c), "Characterization of stress-strain relationships of elastoplastic materials: An improved method with conical and pyramidal indenters", *Mech. Mater.*, **54**, 113-123. http://doi.org/10.1016/j.mechmat.2012.07.006.
Meguid, S., Shagal, G. and Stranart, J. (2002), "3D FE analysis of peening of strain-rate sensitive materials using multiple impingement model", *Int. J. Impact Eng.*, **27**(2), 119-134. https://doi.org/10.1016/S0734-743X(01)00043-4.
Misra, R., Venkatsurya, P., Wu, K. and Karjalainen, L. (2013), "Ultrahigh strength martensite-austenite dual-phase steels with ultrafine structure: the response to indentation experiments", *Mater. Sci. Eng. A*, **560**, 693-699. https://doi.org/10.1016/j.msea.2012.10.015.
Ning, J., Nguyen, V., Huang, Y., Hartwig, K.T. and Liang, S.Y. (2018), "Inverse determination of Johnson-Cook model constants of ultra-fine-grained titanium based on chip formation model and iterative gradient search", *Int. J. Adv. Manuf. Technol.*, **99**, 1131-1140. https://doi.org/10.1007/s00170-018-2508-6.
Noii, N. and Aghayan, I. (2019), "Characterization of elastic-plastic coated material properties by indentation techniques using optimisation algorithms and finite element analysis", *Int. J. Mech. Sci.*, **152**, 465-480. https://doi.org/10.1016/j.ijmecsci.2019.01.010.
Oliver, W. and Pharr, G. (1992), "An improved technique for determining hardness and elastic modulus using load and displacement sensing indentation experiments", *J. Mater. Res.*, **7**(6), 1564-1583. https://doi.org/10.1557/JMR.1992.1564.
Pelletier, H., Krier, J., Cornet, A. and Mille, P. (2000), "Limits of using bilinear stress]strain curve for finite element modeling of nanoindentation response on bulk materials", *Thin Solid Films*, **379**(1-2), 147-155. https://doi.org/10.1016/S0040-6090(00)01559-5.
Qi, K., Zhou, Q. and Yang, W. (2022), "Impact Contact mechanical Performance evaluation of coated medium by semi-analytical method", *Int. J. Solids Struct.*, **444**(25), 128689. https://doi.org/10.1016/j.surfcoat.2022.128689
Qi, K., Zhou, Q., Yang, W. and Yang, J. (2023) "A semi-analytical approach for elastoplastic impact-contact involving coated medium", *Int. J. Solids Struct.*, **283**(1), 112467. https://doi.org/10.1016/j.ijsolstr.2023.112467
Sajadifar, S. and Yapici, G. (2015), "High temperature flow response modeling of ultra-fine grained titanium", *Metals*, **5**(3), 1315-1327. https://doi.org/10.3390/met5031315.
Sakharova, N., Fernandes, J., Antunes, J. and Oliver, W. (2009), "Comparison between Berkovich, Vickers and conical indentation tests: a three-dimensional numerical simulation study", *Int. J. Solids Struct.*, **46**(5), 1095-1104. https://doi.org/10.1016/j.ijsolstr.2008.10.032.
Seo, S., Min, O. and Yang, H. (2005), "Constitutive equation for Ti-6Al-4V at high temperatures measured using the SHPB technique", *Int. J. Impact Eng.*, **31**(6), 735-754. https://doi.org/10.1016/j.ijimpeng.2004.04.010.
Sherafatnia, K., Farrahi, G., Mahmoudi, A. and Ghasemi, A. (2016), "Experimental measurement and analytical determination of shot peening residual stresses considering friction and real unloading behavior", *Mater. Sci. Eng.*, **657**, 309-321. https://doi.org/10.1016/j.msea.2016.01.070.
Soyama, H. and Takeo, F. (2020), "Effect of various peening methods on the fatigue properties of titanium alloy Ti6Al4V

manufactured by direct metal laser sintering and electron beam melting", *Materials*, **13**, 2216. https://doi.org/10.3390/ma13102216

Stauss, S., Schwaller, P., Bucaille, J.L., Rabe, R., Rohr, L., Michler, J. and Blank, E. (2003), "Determining the stress-strain behaviour of small devices by nanoindentation in combination with inverse methods", *Microelectr. Eng.*, **67-68**, 818-825. https://doi.org/10.1016/s0167-9317(03)00192-8.

Swietlicki, A., Szala, M. and Walczak, M. (2022), "Effects of shot peening and cavitation peening on properties of surface layer of metallic materials—A short review", *Materials*, **15**, 2476. https://doi.org/10.3390/ma15072476

Umbrello, D. (2008), "Finite element simulation of conventional and high speed machining of Ti6Al4V alloy", *J. Mater. Proc. Technol.*, **196**(1-3), 79-87. https://doi.org/10.1016/j.jmatprotec.2007.05.007.

Vaidyanathan, R., Dao, M., Ravichandran, G. and Suresh, S. (2001), "Study of mechanical deformation in bulk metallic glass through instrumented indentation", *Acta Mater.*, **49**(18), 3781-3789. http://doi.org/10.1016/S1359-6454(01)00263-4.

Wang, J.S., Zheng, X.J., Zheng, H., Song, S.T. and Zhu, Z. (2010), "Identification of elastic parameters of transversely isotropic thin films by combining nanoindentation and FEM analysis", *Comput. Mater. Sci.*, **49**, 378-385. http://doi.org/10.1016/j.commatsci.2010.05.025.

Wang, Y., Cheng, J., Yang, H. and Zhang, C. (2018), "Numerical study of mechanical response of pure titanium during shot peening", *IOP Conf. Series Mater. Sci. Eng.*, **362**(1), 012009. https://doi.org/10.1088/1757-899X/362/1/012009.

Wen, W., Becker A. and Sun W. (2017), "Determination of material properties of thin films and coatings using indentation tests: A review", *J. Mater. Sci.*, **52**(21), 12553-12573. https://doi.org/10.1007/s10853-017-1348-3.

Yang, H. and Wang, Y. (2018), "Analysis of deformation and texture gradient in shot peened pure titanium", *IOP Conf. Series Mater. Sci. Eng.*, **409**(1), 012017. https://doi.org/10.1088/1757-899X/409/1/012017.

Zhang, K., Jianxin, D., Shuting, L. and Xiaoming, Y. (2016), "Effect of micro/nano-textures and burnished MoS2 addition on the tribological properties of PVD TiAlN coatings against AISI 316 stainless steel", *Surface Coatings Technol.*, **291**, 382-395. https://doi.org/10.1016/j.surfcoat.2016.03.008.

Zhan, H., Wang, G., Kent, D. and Dargusch, M. (2014), "Constitutive modelling of the flow behaviour of a β titanium alloy at high strain rates and elevated temperatures using the Johnson-Cook and modified Zerilli-Armstrong models", *Mater. Sci. Eng. A*, **612**, 71-79. http://doi.org/10.1016/j.msea.2014.06.030.

CC